

# Optimum conditions for synthesizing Fe substituted hibonite

H. Nagumo, K. Kakizaki, and K. Kamishima

Graduate School of Science and Engineering, Saitama University, 255 Shimo-Okubo, Saitama 338-0825, Japan

We investigated the synthesis conditions and magnetic properties of Fe substituted hibonite with initial compositions of  $\text{CaAl}_x\text{Fe}_{y-x}\text{O}_{19}$  ( $1 \leq x \leq 3$ ,  $5 \leq y \leq 9$ ) and  $\text{CaAl}_x\text{Fe}_{8-x}\text{O}_{19}$  ( $0.5 \leq x \leq 1.6$ ) sintered at 1200–1300°C. The optimum conditions for synthesizing the best magnetic hibonite were found to be the initial composition of  $\text{Ca}:\text{Al}:\text{Fe} = 1:0.6:7.4$  and the sintering temperature of 1250°C. The best magnetic hibonite was magnetized at  $75.0 \text{ A}\cdot\text{m}^2/\text{kg}$  at  $T = 5 \text{ K}$  and  $\mu_0 H = 7 \text{ T}$ . This magnetic moment can be interpreted with a model of the collinear magnetic structure. The Curie temperature of the best magnetic hibonite was 330°C, which was the highest among those of iron-substituted hibonite samples.

**Keywords:** M-type, hexaferrite

## 1. Introduction

Ca-based M-type ferrite has been attracting a lot of interest because the other alkaline-earth-based M-type ferrites (Ba, Sr) $\text{Fe}_{12}\text{O}_{19}$  have been used as a permanent magnet for a long time.<sup>1-3)</sup> In spite that pure M-type  $\text{CaFe}_{12}\text{O}_{19}$  phase does not exist in the  $\text{CaO}\text{-Fe}_2\text{O}_3$  diagram,<sup>4,6)</sup> the M-type phase becomes stable with the addition of a rare-earth element of lanthanum to  $\text{CaFe}_{12}\text{O}_{19}$ .<sup>7,8)</sup> The optimum synthesis condition of the (Ca,La)-based M-type ferrite with the highest magnetization was recently clarified.<sup>9)</sup>

Resources of rare-earth elements are, however, limited in comparison with those of the other elements of calcium, iron, and oxygen. Therefore, it is desirable to avoid the use of rare-earth elements in the material.

On the other hand, the crystal structure of M-type ferrite is similar to that of hibonite ( $\text{CaAl}_{12}\text{O}_{19}$ ). Therefore, instead of lanthanum, aluminum can stabilize the M-type structure even with iron elements. This approach is consistent with “element strategy” because aluminum, calcium, iron, and oxygen are abundant elements in Earth's crust.<sup>10)</sup>

We previously reported the study of synthesis and magnetic properties of Fe substituted hibonite.<sup>11)</sup> In this report, we changed initial composition from  $\text{CaAl}_{12-x}\text{Fe}_x\text{O}_{19}$  to  $\text{CaAl}_{10-x}\text{Fe}_x\text{O}_{19}$ , in order to prevent the excess of  $\alpha\text{-Fe}_2\text{O}_3$  and to improve the magnetic properties. But it was insufficient to optimize synthesis conditions because  $\alpha\text{-Fe}_2\text{O}_3$  still remained in the magnetic samples of  $\text{CaAl}_{10-x}\text{Fe}_x\text{O}_{19}$ .

In this study, we have investigated the optimum synthesis conditions and magnetic properties of Fe substituted hibonite in order to produce a rare-earth-free Ca-based ferromagnet.

## 2. Experimental procedure

Samples were prepared by a conventional ceramic method. We used  $\text{CaCO}_3$ ,  $\text{Al}_2\text{O}_3$ , and  $\alpha\text{-Fe}_2\text{O}_3$  as starting

materials. First,  $\text{Al}_2\text{O}_3$  powder was heated at 500°C for an hour in order to remove water molecules on the material. The starting materials were mixed in the desired proportions of  $\text{CaAl}_x\text{Fe}_{y-x}\text{O}_{19}$  ( $1 \leq x \leq 3$ ,  $5 \leq y \leq 10$ ) and  $\text{CaAl}_{8-x}\text{Fe}_x\text{O}_{19}$  ( $6.4 \leq x \leq 7.5$ ) in a ball-milling pot for 24 h. The mixed powder was pressed into a disk shape. The disk was pre-sintered in air at 900°C for 5 h. The sintered sample was pounded in a mortar and then ground into fine powder using a planetary ball mill for 10 minutes at 1100 rpm (Fritsch, P-7 Premium line). The powder was pressed into a disk shape again. The disks were heated at 1100–1400°C for 5 h. X-ray diffraction (XRD) analysis with  $\text{Cu-K}\alpha$  radiation was performed to characterize the crystalline samples. The magnetic properties were measured by using a vibrating sample magnetometer (Tamakawa TM-VSM2130HGC) and superconducting quantum interference device (SQUID) magnetometers (Quantum Design MPMS-XL). The chemical composition was examined through energy dispersive X-ray analysis (EDX).

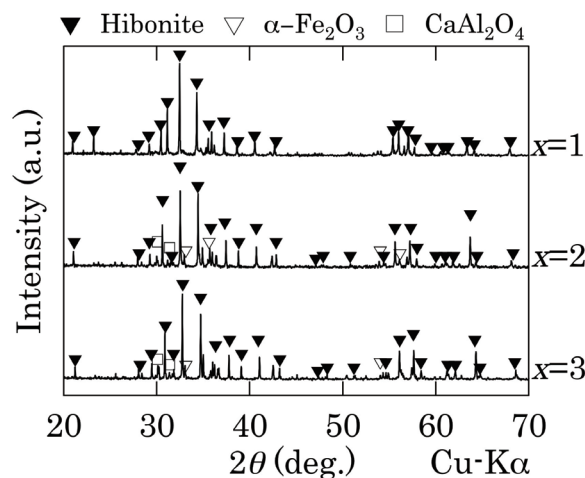


**Fig. 1** X-ray diffraction patterns of initial composition samples of  $\text{CaAl}_x\text{Fe}_{y-x}\text{O}_{19}$  ( $1 \leq x \leq 3$ ,  $y = 8$ ) sintered at  $T_s = 1300^\circ\text{C}$ .

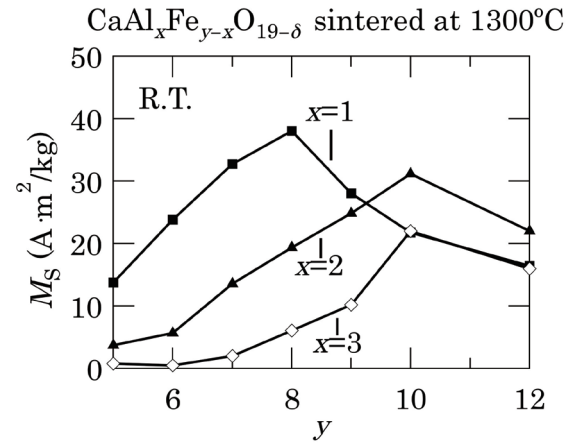
### 3. Results and discussion

Figure 1 shows the X-ray diffraction patterns of the Ca:Al:Fe = 1:x:y-x ( $1 \leq x \leq 3$ ,  $y = 8$ ) composition samples sintered at  $T_s = 1300^\circ\text{C}$ . The sample with the initial composition at  $x = 1$  and  $y = 8$  showed the single hibonite phase. The diffraction pattern of hibonite is almost identical to that of Sr-based M-type ferrite. The other samples of  $x = 2$  and 3 contained minority phases of  $\alpha\text{-Fe}_2\text{O}_3$  and  $\text{CaAl}_2\text{O}_4$  although the main phase was that of hibonite. This situation is same for other starting composition samples with Ca:Al:Fe = 1:x:y-x ( $1 \leq x \leq 3$ ,  $5 \leq y \leq 9$ ). But the single hibonite phase was observed only for the sample at  $x = 1$  and  $y = 8$ .

Figure 2 shows the room-temperature saturation magnetization ( $M_s$ ) of initial composition samples of  $\text{CaAl}_x\text{Fe}_{y-x}\text{O}_{19-\delta}$  ( $1 \leq x \leq 3$ ,  $5 \leq y \leq 12$ ) sintered at  $T_s = 1300^\circ\text{C}$ , where  $M_s$  was estimated from the magnetization measurements at  $-2 \text{ T} \leq \mu_0 H \leq 2 \text{ T}$ . The sample at  $x = 1$  and  $y = 8$  had the highest  $M_s$  among these samples. This is consistent with the fact that the sample at  $x = 1$  and  $y = 8$  contained no minority phases of  $\alpha\text{-Fe}_2\text{O}_3$  and  $\text{CaAl}_2\text{O}_4$ .

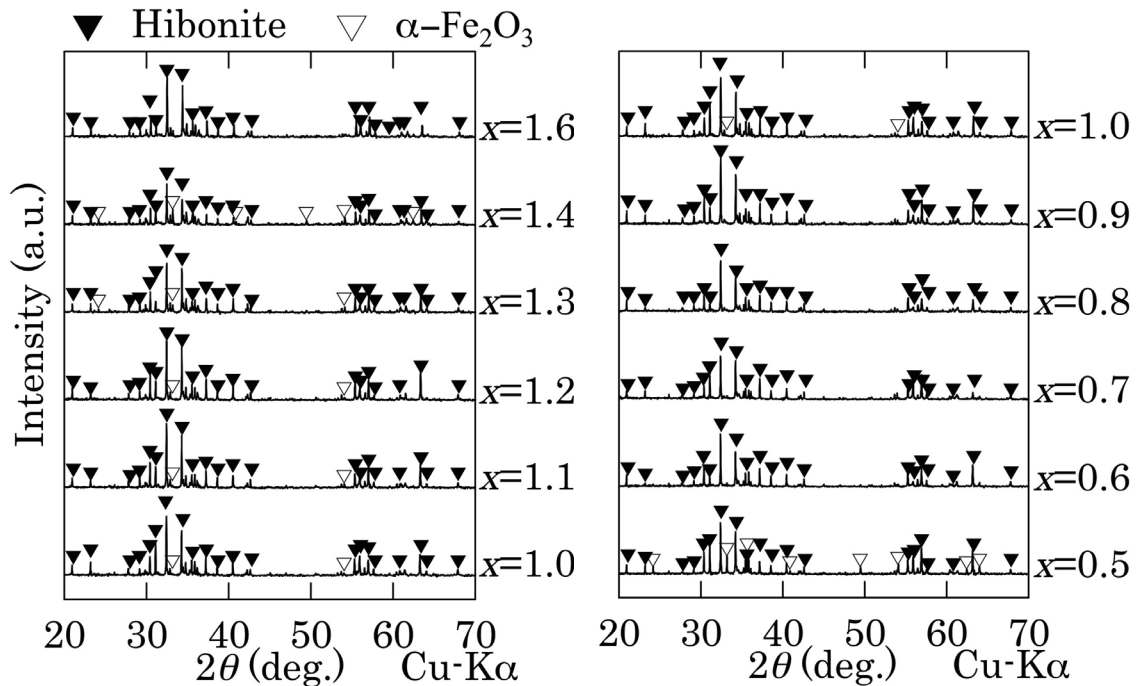
These experimental results of  $\text{CaAl}_x\text{Fe}_{y-x}\text{O}_{19-\delta}$  strongly suggest that the suitable (Al+Fe)/Ca ratio is 8 for the formation of the iron-substituted magnetic hibonite. This led us to the next experiments to determine the optimum Al:Fe ratio so as to synthesize the best magnetic hibonite with the highest magnetization and the highest Curie temperature.

Figure 3 shows the X-ray diffraction patterns of initial composition samples of  $\text{CaAl}_x\text{Fe}_{8-x}\text{O}_{19-\delta}$  ( $0.5 \leq x \leq$



**Fig. 2** Room-temperature saturation magnetization of initial composition samples of  $\text{CaAl}_x\text{Fe}_{y-x}\text{O}_{19-\delta}$  ( $1 \leq x \leq 3$ ,  $0 \leq y \leq 12$ ) sintered at  $T_s = 1300^\circ\text{C}$ .

1.6) sintered at  $T_s = 1250^\circ\text{C}$ . The maximum iron substitution amount corresponds to  $x_{\text{max}} = 0.6$  where the secondary phase of hematite was not left. Here, the sintering temperature  $T_s$  was decreased to  $1250^\circ\text{C}$  from  $1300^\circ\text{C}$  because the samples sintered at  $T_s = 1300^\circ\text{C}$  showed the secondary hematite phase at  $x < 1.0$ . High  $T_s$  can remove iron and calcium elements from the hibonite structure with high concentration of  $\text{Fe}^{3+}$ , possibly due to a low melting point of  $\text{CaFe}_2\text{O}_4$ . On the other hand, the single hibonite phase was not observed for the samples at  $T_s \leq 1225^\circ\text{C}$ , suggesting the lowest limit of  $T_s$  for the formation of the single phase of hibonite.



**Fig. 3** X-ray diffraction patterns of initial composition samples of  $\text{CaAl}_x\text{Fe}_{8-x}\text{O}_{19-\delta}$  ( $0.5 \leq x \leq 1.6$ ) sintered at  $T_s = 1250^\circ\text{C}$ .

Figure 4 shows the lattice constants of the hibonite phase in initial composition samples of  $\text{CaAl}_x\text{Fe}_{8-x}\text{O}_{19-\delta}$  ( $0.5 \leq x \leq 1.6$ ) sintered at  $T_s = 1250^\circ\text{C}$ . The lattice constants of  $a$  and  $c$  were obtained by the use of Cohen's least square method.<sup>12)</sup> Both  $a$  and  $c$  became maximum at  $x = 0.6$ , which is in agreement with the above-mentioned  $x_{\text{max}}$ . The maximum lattice constants at  $x = 0.6$  implied that  $\text{Fe}^{3+}$  ions maximally replaced  $\text{Al}^{3+}$  ions in the hibonite structure because the ionic radius of an  $\text{Fe}^{3+}$  ion  $r[\text{Fe}^{3+}]$  is larger than that of an  $\text{Al}^{3+}$  ion  $r[\text{Al}^{3+}]$ .

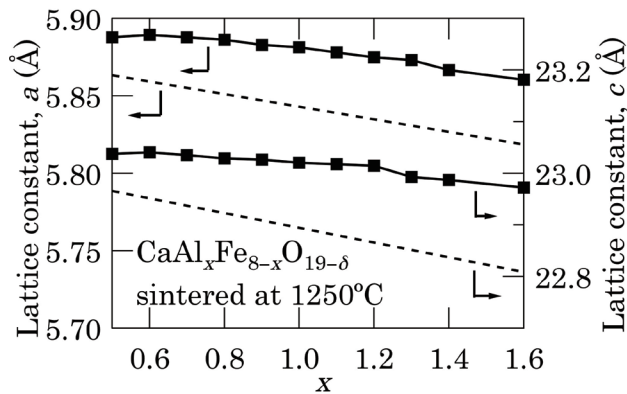


**Fig. 4** Lattice constants of initial composition samples of  $\text{CaAl}_x\text{Fe}_{8-x}\text{O}_{19-\delta}$  ( $0.5 \leq x \leq 1.6$ ) sintered at  $T_s = 1250^\circ\text{C}$ . Dotted lines are connected between lattice constants of  $\text{CaAl}_{12}\text{O}_{19}$  at  $x = 8$  and those of  $\text{SrFe}_{12}\text{O}_{19}$  (instead of  $\text{CaFe}_{12}\text{O}_{19}$  that does not exist) at  $x = 0$ , where a conversion of  $x = 8x' / 12$  is employed for  $\text{CaAl}_{12-x'}\text{Fe}_{x'}\text{O}_{19}$  due to the change of  $(\text{Al}+\text{Fe})/\text{Ca}$  from 12 to 8.

Figure 5 shows the room-temperature saturation magnetization ( $M_s$ ), the Curie temperature ( $T_C$ ) and the relative intensity  $I_{(102)}^{\alpha\text{-Fe}_2\text{O}_3} / I_{(203)}^{\text{hibonite}}$  of initial composition samples of  $\text{CaAl}_x\text{Fe}_{8-x}\text{O}_{19-\delta}$  ( $0.5 \leq x \leq 1.6$ ). With decreasing  $x$  from 1.6,  $T_C$  was linearly increased up to  $330^\circ\text{C}$  at  $x = 0.6$  and then slightly decreased at  $x = 0.5$ . This  $x$  dependence of  $T_C$  is comparable to the variation of the lattice constants as shown in Fig. 4. The highest  $T_C$  strongly suggests that the sample with  $x = 0.6$  sintered at  $1250^\circ\text{C}$  contains the maximum amount of iron cations in the hibonite structure. Also,  $M_s$  was basically increased with decreasing  $x$  from 1.6 to 0.6 except that  $M_s$  deviated from this linear tendency at  $x = 1.4$  and 1.3 because of the formation of a minority phase of  $\alpha\text{-Fe}_2\text{O}_3$ . The sample with  $x = 0.6$  had the maximum  $M_s$  of  $44 \text{ A m}^2/\text{kg}$  and the highest  $T_C$  of  $330^\circ\text{C}$ .

The EDX analysis of the sample with  $x = 0.6$  provides the result of  $\text{Ca}:\text{Al}:\text{Fe} = 1.00 \pm 0.04 : 0.62 \pm 0.04 : 7.81 \pm 0.23$  (average value  $\pm$  one sigma estimation). The composition of Fe is slightly larger than the initial amount, which may be caused by low-melting-point calcium-iron oxides such as  $\text{CaFe}_2\text{O}_4$  that can be eluted off from the hibonite grain. The chemical formula of this sample can be expressed as  $\text{CaAl}_{0.6}\text{Fe}_{7.8}\text{O}_{13.6}$  where the

composition ratio of oxygen is estimated from the charge balance with the concentration of  $\text{Ca}^{2+}$ ,  $\text{Al}^{3+}$ , and  $\text{Fe}^{3+}$  cations. The form of this chemical formula is much different from the reference materials of hibonite ( $\text{CaAl}_{12}\text{O}_{19}$ ) and M-type ferrite ( $\text{SrFe}_{12}\text{O}_{19}$ ).

On the other hand, the  $x$  dependences of the lattice constants are similar to the dotted lines connected between lattice constants of  $\text{CaAl}_{12}\text{O}_{19}$  and those of  $\text{SrFe}_{12}\text{O}_{19}$  as shown in Fig. 4. This fact suggests that the framework of the hibonite structure is maintained even in the change of  $(\text{Al}+\text{Fe})/\text{Ca}$  ratio. The crystal structure consists of a close-packed framework of large ions ( $\text{Ca}^{2+}$  and  $\text{O}^{2-}$ ) with intervening small ions ( $\text{Al}^{3+}$  and  $\text{Fe}^{3+}$ ). Therefore, we can assume that the total number of large ions ( $\text{Ca}^{2+}$  and  $\text{O}^{2-}$ ) in the hibonite structure is kept at 20 ( $= 1+19$ ). Based on this assumption, the chemical formula of the sample with  $x = 0.6$  is estimated to be  $\text{Ca}_{1.4}\text{Al}_{0.8}\text{Fe}_{10.7}\text{O}_{18.6}$ . The total number of  $\text{Al}^{3+}$  and  $\text{Fe}^{3+}$  cations becomes 11.5 that is smaller than 12.

This picture can be applied to the case of Al-substituted (Ca,La)-based M-type ferrite. Shigemura *et al.* recently reported that the Curie temperature of  $\text{Ca}_{0.88}\text{La}_{0.12}\text{Fe}_{8.80}\text{Al}_{1.01}\text{O}_{15.8}$  was about  $350^\circ\text{C}$ .<sup>13)</sup> This chemical formula can be converted to  $\text{Ca}_{1.05}\text{La}_{0.14}\text{Fe}_{10.5}\text{Al}_{1.20}\text{O}_{18.8}$  on the assumption that the total number of large ions ( $\text{Ca}^{2+}$ ,  $\text{La}^{3+}$ , and  $\text{O}^{2-}$ ) is kept at 20. The estimated amounts of  $\text{Fe}^{3+}$  in chemical formulas

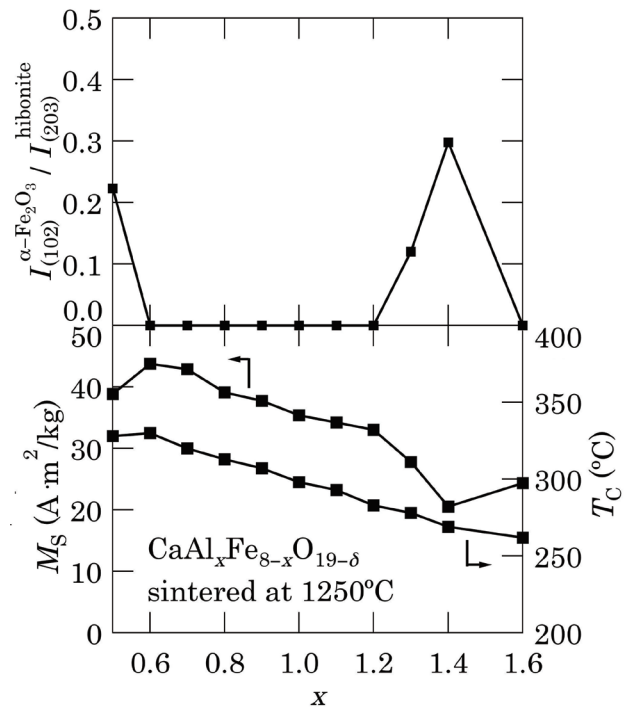


**Fig. 5** Room-temperature saturation magnetization ( $M_s$ ) and Curie temperature ( $T_C$ ) of initial composition samples of  $\text{CaAl}_x\text{Fe}_{8-x}\text{O}_{19-\delta}$  ( $0.5 \leq x \leq 1.6$ ) sintered at  $T_s = 1250^\circ\text{C}$ . Intensity ratio of  $\alpha\text{-Fe}_2\text{O}_3$  (102) plane to hibonite (203) plane is also shown.

are similar between  $\text{Ca}_{1.4}\text{Al}_{0.8}\text{Fe}_{10.7}\text{O}_{18.6}$  and  $\text{Ca}_{1.05}\text{La}_{0.14}\text{Fe}_{10.5}\text{Al}_{1.20}\text{O}_{18.8}$ , which may cause the similarity in the Curie temperature.

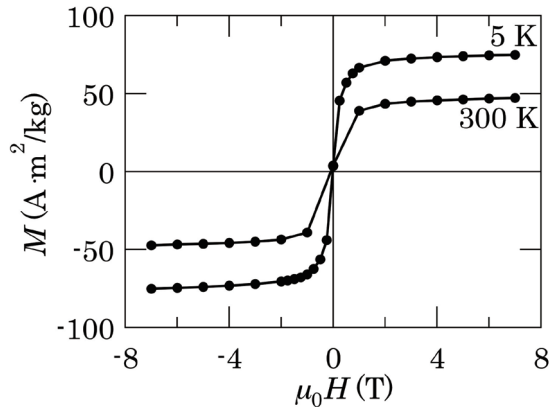


**Fig. 6** Magnetization curves at  $T = 5$  K and 300 K for sample at  $x = 0.6$  sintered at  $T_s = 1250^\circ\text{C}$ .

Figure 6 shows the magnetization curves at  $T = 5$  K and 300 K for the sample with  $x = 0.6$  sintered at  $T_s = 1250^\circ\text{C}$ . Gradual increase of magnetization was observed above  $\mu_0 H > 2$  T. At the maximum external magnetic field of  $\mu_0 H = 7$  T, the magnetizations at  $T = 5$  K and 300 K are  $75.0 \text{ A}\cdot\text{m}^2/\text{kg}$  and  $47.3 \text{ A}\cdot\text{m}^2/\text{kg}$ , respectively. The magnetization at  $T = 5$  K corresponds to the magnetic moment per formula unit of  $13.1 \mu_B/\text{f.u.}$

We would like to discuss the magnetic structure of the best magnetic hibonite in our study. The magnetic structure of this iron-substituted hibonite can be similar to that of the M-type ferrite because the crystal structure of hibonite is similar to that of the M-type ferrite. The M-type ferrite has a collinear magnetic structure where eight of the  $\text{Fe}^{3+}$  cations are antiparallel to the other four  $\text{Fe}^{3+}$  cations. The total magnetic moment of the M-type ferrite is equivalent to four  $\text{Fe}^{3+}$  cations ( $20 \mu_B$ ).

Here, the chemical formula of the best magnetic hibonite is estimated to be  $\text{Ca}_{1.4}\text{Al}_{0.8}\text{Fe}_{10.7}\text{O}_{18.6}$ . Albanese demonstrated that  $\text{Al}^{3+}$  cations in  $\text{BaAl}_x\text{Fe}_{12-x}\text{O}_{19}$  tend to occupy the up-spin 12k site at  $x \leq 1$ .<sup>14</sup> Also, the estimated chemical formula with the excess of  $\text{Ca}^{2+}$  cations suggests that  $\text{Ca}^{2+}$  replaces  $\text{O}^{2-}$  (possibly in the R-block), which can produce vacancy at a small cation site due to the local electroneutrality (the Pauling principle). Therefore, we can assume that the magnetic hibonite has the collinear magnetic structure where the up-spin-sites contain 0.8  $\text{Al}^{3+}$  and 0.5 vacancy. Then, 6.7  $\text{Fe}^{3+}$  cations are antiparallel to the other four  $\text{Fe}^{3+}$  cations. The total magnetic moment of the magnetic hibonite becomes equivalent to 2.7  $\text{Fe}^{3+}$  cations ( $13.5 \mu_B$ ). This value is close to the experimental result of  $13.1 \mu_B/\text{f.u.}$  at  $T = 5$  K and  $\mu_0 H = 7$  T.

The slight difference between the experimental result and the estimated value can be caused by the deviation from the collinear magnetic structure. In fact,

Batlle *et al.* pointed out that the substitution of  $\text{Co}^{2+}\text{-Ti}^{4+}$  for  $\text{Fe}^{3+}$  in  $\text{BaFe}_{12}\text{O}_{19}$  can progressively break the collinearity of the magnetic structure of  $\text{BaFe}_{12-2x}\text{Co}_x\text{Ti}_x\text{O}_{19}$  at  $x > 0.7$  although the overall behavior remains ferrimagnetic.<sup>15</sup> In our case, the collinearity of our sample can be also weakened because the estimated amount of the  $\text{Fe}^{3+}$  cations in our sample is close to this threshold of  $10.6 (= 12-2 \times 0.7)$  and our sample does not contain magnetic  $\text{Co}^{2+}$  cations. The high-field susceptibility of our sample is relatively high as shown in Fig. 6, suggesting the weakened collinearity.

Therefore, our result is consistent with the previous studies of M-type ferrite.

#### 4. Conclusion

We have successfully synthesized  $\text{Fe}^{3+}$  substituted hibonite-phase samples by a conventional ceramic method. The optimum synthesis conditions of the best magnetic hibonite are found to be the initial composition of  $\text{Ca}:\text{Al}:\text{Fe} = 1:0.6:7.4$  and the sintering temperature of  $1250^\circ\text{C}$ . The magnetization of the best magnetic hibonite was  $75.0 \text{ A}\cdot\text{m}^2/\text{kg}$  at  $T = 5$  K and  $\mu_0 H = 7$  T. This magnetic moment can be basically interpreted with the model of the collinear magnetic structure. The Curie temperature of the best magnetic hibonite was  $330^\circ\text{C}$ , which is the highest among those of iron-substituted hibonite samples.

#### References

- 1) J. Smit and H. P. J. Wijn: Ferrites, pp. 182–184, pp. 193–194 (Philips Technical Library, Netherlands 1959).
- 2) S. Chikazumi: Physics of Ferromagnetism, p. 210 (Oxford University Press, Oxford, 2009).
- 3) Ü. Özgür, Y. Alivov, and H. Morkoc: *J. Mater. Sci-Mater. EL.*, **20**, 789 (2009).
- 4) B. S. Boyanov: *J. Min. Met.*, **41 B**, 67 (2005).
- 5) M. Hillert, M. Selleby, and B. Sundman: *Metall. Trans. A*, **21A**, 2759 (1990).
- 6) B. Philips and A. Muan: *J. Am. Ceram. Soc.*, **41**, 445 (1958).
- 7) N. Ichinose and K. Kurihara: *J. Phys. Soc. Jpn.*, **18**, 1700 (1963).
- 8) H. Yamamoto, T. Kawaguchi, and M. Nagakura: *IEEE Trans. Magn.*, **15**, 1141 (1979).
- 9) M. Shigemura, K. Watanabe, K. Kakizaki, and K. Kamishima: *J. Magn. Soc. Jpn.*, **41**, 10 (2017).
- 10) F. W. Clarke and H. S. Washington: The Composition of the Earth's Crust, pp. 20–21 (United States Geological Survey, Washington, 1924).
- 11) H. Nagumo, K. Watanabe, K. Kakizaki and K. Kamishima: *J. Magn. Soc. Jpn.*, **41**, 20 (2017).
- 12) B. D. Cullity: Elements of X-ray Diffraction, 342 (Addison-Wesley, 1967).
- 13) M. Shigemura, K. Kakizaki, and K. Kamishima: *J. Magn. Soc. Jpn.*, **41**, 94 (2017).
- 14) G. Albanese: *J. Magn. Mater.*, **147**, 421 (1995).
- 15) X. Batlle, X. Obradors, J. Rodríguez-Carvajal, M. Pernet, M. V. Cabañas, M. Vallet: *J. Appl. Phys.*, **70**, 1614 (1991).

Received Jun. 18, 2017; Revised Aug. 8, 2017; Accepted Oct. 30, 2017